



# Human Kidney Stone Analysis using X-ray Powder Diffraction

Alok K. Mukherjee

**Abstract** | Physical and chemical methods available for kidney stone analysis are critically reviewed. Although various methods, such as the FTIR and Raman spectroscopy, scanning electron microscopy, thermogravimetry etc. can be used for qualitative phase analysis of kidney stones, the Rietveld method based on high quality X-ray powder diffraction data provides a precise and reliable technique for identifying the structure as well as the quantitative phase abundance of different crystalline components in human urinary calculi. Quantitative phase analyses of ten (10) kidney stones (KS1-KS10) from eastern India revealed that most of the calculi samples are mixture of phases with calcium oxalate monohydrate (whewellite) as the major constituent and varying amounts of calcium oxalate dihydrate (weddellite), calcium hydroxyapatite, uric acid and ammonium acid urate. The crystal structures of whewellite and weddellite have been redetermined using X-ray powder diffraction methodology.

## 1 Introduction

Pathological calcification in hollow organs or ducts of human body, for example, stone formation in the urinary tract (kidney, ureter and bladder), constitutes a major medical problem and has been affecting an increasing number of people around the world.<sup>1-3</sup> Apart from substantial suffering and associated morbidity, the deposition of minerals or organic compounds in the urinary system, commonly called urinary/renal calculi or kidney stones can result in several conditions, ranging from poor voiding to renal dysfunction. The demographic distribution of a population susceptible to kidney-stone induced problems varies around the world. For example, in the US and developed countries in Europe about 10–15% of the total population experience kidney-stone related problems at some point of their lives.<sup>4-6</sup> In the Indian sub-continent and some parts of South America, kidney-stone formation affects up to 25% of the population.<sup>7,8</sup> Urinary calculi are solid concretions resulting from a transient, intermittent or permanent disorder in urine composition that induces urine super-saturation. Various causes such as metabolic disorder, dietary habit including fluid intake, water quality, climate and urinary tract infection have been cited as the reasons for

the high prevalence of kidney stone disease in some countries, but no consensus has been reached.<sup>9-11</sup> A positive correlation between obesity and the risk of kidney-stone formation has also been reported.<sup>12-14</sup> From a medical point of view, different aspects of calcification must be taken into consideration to establish a meaningful correlation between stone formation and the disease. These include chemical diversity, morphological features at the mesoscopic and macroscopic scale, presence of trace elements and functional groups, such as carbonate groups in hydroxyapatite, and proteins. Although kidney-stones can be removed in most cases by either invasive or non-invasive clinical or surgical procedures,<sup>15</sup> it is not possible to prevent their recurrence. Without adequate follow-up measures, the recurrence rate of stone formation can be as high as 30–50%.<sup>16</sup> In this context, knowledge of composition and quantification of kidney-stones is of fundamental importance for understanding the causes that led to their formation, the conditions of their nucleation and growth, and the existence of particular lithogenic processes, which in turn would help in the development of prophylactic measures.<sup>17-20</sup>

The present review focuses on the quantitative phase analysis and structural characterization

Department of Physics,  
Jadavpur University,  
Jadavpur,  
Kolkata 700 032, India.  
akm\_ju@rediffmail.com

of constituent phases in kidney stones using the Rietveld-based refinement technique with powder X-ray diffraction (PXRD) data. The principles of methodology used for such analyses have also been discussed.

## 2 Chemical Diversity of Kidney Stones

The composition of urinary calculi is complex and diverse, and can be divided into two parts, an organic matrix containing mainly proteins, lipids, carbohydrates, cholesterol, uric acid and bio-minerals. Different chemical phases can be identified inside or at the surface of the kidney stones. The identification of crystalline phases in urinary calculi is of key importance because they are related with distinct bio-chemical conditions during their formation. Over sixty five (65) different molecules have been identified in urinary calculi.<sup>3,17</sup> These molecules, which correspond to their chemical composition, can crystallize in more than eighty (80) different crystalline phases. It is found that calcium is present in numerous mineral phases in urinary calculi such as whewellite [calcium oxalate monohydrate (COM),  $\text{CaC}_2\text{O}_4 \cdot \text{H}_2\text{O}$ ], weddellite [calcium oxalate dihydrate (COD),  $\text{CaC}_2\text{O}_4 \cdot 2\text{H}_2\text{O}$ ], caoxite [calcium oxalate trihydrate (COT),  $\text{CaC}_2\text{O}_4 \cdot 3\text{H}_2\text{O}$ ], brushite [calcium hydrogen phosphate dihydrate (BRS),  $\text{CaHPO}_4 \cdot 2\text{H}_2\text{O}$ ], hydroxyapatite [calcium hydroxyapatite (APP),  $\text{Ca}_{10}(\text{PO}_4)_6(\text{OH})_2$ ], carbonatedapatite [calcium hydroxyapatite carbonate (HAC),  $\text{Ca}_{10}(\text{PO}_4\text{CO}_3)_6(\text{OH})_8$ ] and whitlockite [tricalcium phosphate (WHT),  $\text{Ca}_3(\text{PO}_4)_2$ ]. Other mineral phases found in kidney stones include struvite [magnesium ammonium phosphate hexahydrate (STV),  $\text{MgNH}_4\text{PO}_4 \cdot 6\text{H}_2\text{O}$ ], dittmarite [magnesium ammonium phosphate monohydrate (MPM),  $\text{MgNH}_4\text{PO}_4 \cdot \text{H}_2\text{O}$ ] and newberyite [magnesium hydrogen phosphate trihydrate (MPT),  $\text{MgHPO}_4 \cdot 3\text{H}_2\text{O}$ ]. Organic compounds such as anhydrous uric acid (UAA,  $\text{C}_5\text{H}_4\text{N}_4\text{O}_3$ ), uric acid dihydrate (UAD,  $\text{C}_5\text{H}_4\text{N}_4\text{O}_3 \cdot 2\text{H}_2\text{O}$ ), cholesterol, cystine (CYS,  $\text{C}_6\text{H}_{12}\text{N}_2\text{O}_4\text{S}_2$ ), xanthine (XAN,  $\text{C}_5\text{H}_5\text{N}_4\text{O}_2$ ), sodium acid urate (SAU,  $\text{NaC}_5\text{H}_3\text{N}_4\text{O}_3 \cdot \text{H}_2\text{O}$ ) and ammonium acid urate (AAU,  $\text{NH}_4\text{C}_5\text{H}_3\text{N}_4\text{O}_3 \cdot \text{H}_2\text{O}$ ) are also found in urinary stones. Recently a uric acid derivative with the chemical formula  $\text{C}_7\text{H}_8\text{N}_4\text{O}_5$ , has been also reported to be present in kidney stone.<sup>21</sup>

## 3 Methods of Urinary Calculi Analysis

Different chemical and physical methods such as the wet chemical analysis, optical polarizing microscopy, Fourier Transform Infrared (FTIR) and Raman spectroscopy, scanning electron microscopy (SEM) coupled with energy dispersive X-ray analysis (EDX), thermogravimetry (TG) and powder X-ray diffraction (PXRD) can be used for qualitative

and quantitative analyses of urinary calculi.<sup>22–29</sup> The specific property possessed by some ions present in the constituents of the calculus of reacting with a chemical reagent producing the development of a particular colour or characteristic crystalline phase forms the basis of all chemical methods. The chemical analysis is relatively inaccurate because of false positive and false negative results, and does not distinguish between the crystalline phases. The FTIR spectroscopy is based on the study of interaction of a broad band infrared light with the covalent bonds of the compound present in the calculus, leading to the appearance of some characteristic bands that make their identification possible. The vibrational motions of individual chemical bonds for all molecules lie in the wavelength range 2–20  $\mu\text{m}$  corresponding to the wave number range of 5000–500  $\text{cm}^{-1}$ . Since FTIR method is based on vibrational spectroscopy reflecting the molecular structure, it is sensitive to the molecular environment. This method is suitable for determining the chemical composition of urinary calculus. Its main advantages are that it can be applied on very small sample quantity (< 1 mg) and allows the identification of both crystalline and amorphous components (proteins, lipids, amorphous phosphates etc.) of urinary calculi. Raman spectroscopy, which relies on the principle of inelastic scattering of light photons by atom or molecule, also permits evaluation of the structure of components of urinary calculi at the microscopic level.<sup>30</sup> It can identify the vibrational bands specific for the chemical bonds of organic molecules in the range 400–1800  $\text{cm}^{-1}$ . Laser Raman microprobe,<sup>31</sup> which is a combination of a microscope and a Raman spectrometer has also been used to determine the composition of different urinary calculi.<sup>32</sup>

The scanning electron microscope (SEM) images the sample surface with a range of magnifications (100–50000 or more) by scanning it with a high energy beam of electrons. The electrons interact with atoms that make up the calculi samples producing signals containing information about the surface topology of the sample. Such a method also provides information about the nature of crystalline components, shape of the crystals, internal structure, location of components and relation between the crystals and the organic matrix.<sup>33–35</sup> SEM coupled with EDX can give an idea about the percentage composition of each element present in a particular stone.<sup>28</sup> Thermal analysis (TG-DTA) can also be used to identify hydrated oxalates and related minerals in urinary calculi. The TG-DTA could be an alternative method for the characterization of monohydrate and dihydrate of calcium oxalate (whewellite and weddellite) when present together in a kidney stone.<sup>36,37</sup>

#### 4 X-ray Powder Diffraction (PXRD)

X-ray diffraction (XRD) has long been recognized as a powerful method for the determination of phase composition of crystalline material.<sup>38</sup> Most of our knowledge about the structure of material has been obtained by this technique. Among the various physical methods mentioned earlier, X-ray powder diffraction (PXRD) is undoubtedly the optimal technique for the identification as well as quantification of crystalline phases in kidney stones. The X-ray powder profile-fitting structure refinement by the Rietveld method<sup>39-41</sup> is uniquely versatile for quantitative phase analysis in a multi-phase mixture of polycrystalline materials.<sup>41-44</sup> This method can be applied successfully for estimating the quantitative abundance of mineral phases in kidney stones.<sup>45</sup> The Rietveld based methods are able to accurately decouple phases with high degree of reflection overlap and have the potential to produce more reliable results than those obtained from the conventional single peak methods.<sup>46,47</sup> The improvement derives from the fact that all traditional methods of analyzing X-ray powder diffraction patterns use only selective parts of X-ray data, whereas the Rietveld methods utilize the entire diffraction profile during analysis. The impact of some sample related effects, such as preferred orientation, are minimized by the inclusion of entire diffraction pattern. In addition to structural parameters which must be refined to ensure the best fit between the observed and calculated X-ray patterns, other parameters related to micro-structural features, such as crystallite size, strain or preferred orientation, can also be refined during the Rietveld refinement. These factors are important when attempting to elucidate the mechanism for in vivo crystal growth of urinary calculi. It is, however, necessary to emphasize that quantitative phase analysis of kidney stones using the Rietveld method is not straightforward due to the fact that most of the stone samples are crystallographically heterogeneous and the majority of bio-minerals present in the urinary stones have low crystal symmetry (triclinic and monoclinic), which in turn leads to a considerable overlapping of peaks in the X-ray powder diffraction pattern.

#### 5 Mathematical Basis

The profile of an X-ray powder pattern is the result of convolution of a specimen profile (C) and a combined function modelling the aberrations introduced by the diffractometer geometry (A) and wavelength dispersion (W), and can be expressed as

$$y_c(2\theta) = [(W * A) * C](2\theta) + \text{bkg}, \quad (1)$$

where the symbol \* represents the convolution operation and 'bkg' is the background

contribution. The experimental profile can be fitted with a suitable pseudo-Voigt (pV) analytical function<sup>48,49</sup> because it individually takes into account of both the particle size and the strain broadening of experimental profiles.

For both  $K\alpha_1$  and  $K\alpha_2$  profiles, the line broadening function and the symmetric part of instrumental function may be represented by the pseudo-Voigt function (pV), which is the sum of the Gaussian (G) and the Lorentzian (L) components with a mixing factor  $\eta$  ( $\eta = 1$  for L and 0 for G). Due to anisotropy in the particle size and microstrain values, the profiles with different Miller indices are broadened to different extent, and this effect often creates problem during the Rietveld structure refinements. To consider the effect of particle size and microstrain on the profile shape, tensors similar to the temperature factors are frequently used for crystallite size ( $D$ ) and r.m.s. lattice microstrain ( $\langle \epsilon^2 \rangle^{1/2}$ ) in different crystallographic directions:

$$D(h_1, h_2, h_3) = \left( \sum_{ij} D_{ij}^2 h_i h_j / \sum_{ij} \delta_{ij} h_i h_j \right)^{1/2} \quad (2)$$

$$\langle \epsilon^2 \rangle^{1/2}(h_1, h_2, h_3) = \left( \sum_{ij} \langle \epsilon \rangle_{ij}^2 h_i h_j / \sum_{ij} \delta_{ij} h_i h_j \right)^{1/2}, \quad (3)$$

where  $\delta_{ij} = 0$  if  $D_{ij} = 0$  or  $\langle \epsilon \rangle_{ij} = 0$ , and  $\delta_{ij} = 1$  in the other cases.<sup>50</sup>

The quantitative phase abundance of different crystalline components in a mixture of multiphase samples was estimated using the relation

$$w_i = S_i (ZMV)_i / \sum_j S_j (ZMV)_j, \quad (4)$$

where  $w_i$  is the weight fraction of each phase,  $i$  is the value for a particular phase  $j$  among the  $N$  phases,  $S_j$  is the refined scale factor,  $Z$  is the number of formula units per cell,  $M$  is the molecular weight of the formula unit and  $V$  is the volume of the unit cell.<sup>41-43,50</sup>

During the Rietveld refinement, structure parameters (atomic positions, temperature and occupancy factors), scale factor, unit cell parameters and background coefficients, along with the profile parameters describing the peak shapes and widths are varied through a least-squares procedure until the calculated powder pattern best matches the observed pattern. The quantity that is minimized by the least-square procedure is

$$S = \sum_{i=1}^N \omega_i(2\theta) \{y(2\theta_i)_{obs} - y(2\theta_i)_{cal}\}^2, \quad (5)$$

where,  $y(2\theta)_{obs}$  and  $y(2\theta)_{cal}$  are the observed and calculated intensities at the  $i$ th step of the digitized powder pattern, respectively  $\omega_i(2\theta)$  is the appropriate weighting factor and the summation

running over all data points. In general, the weighting factor  $\omega_i(2\theta)$  is set high at the beginning of a refinement when the structure is incomplete or only approximately correct, because the interatomic distances easily become unreasonably long or short at this stage. It can then be reduced during the course of refinement as the structural model improves.

The agreement between the observed and calculated profiles can be assessed using different reliability index parameters,

$$R_p = \sum |y_i(\text{obs}) - y_i(\text{calc})| / \sum |y_i(\text{obs})| \quad (6)$$

$$R_{wp} = [\sum \omega_i \{y_i(\text{obs}) - y_i(\text{calc})\}^2 / \sum \omega_i \{y_i(\text{obs})\}^2]^{1/2} \quad (7)$$

and

$$R_B = \sum |I_K(\text{obs}) - I_K(\text{calc})| / \sum |I_K(\text{obs})| \quad (8)$$

The goodness of fit (GOF) is established by comparing  $R_{wp}$  with the expected error,  $R_{exp}$ ,

$$R_{exp} = [(N - P) / \sum \omega_i \{y_i(\text{obs})\}^2]^{1/2}, \quad (9)$$

where  $N$  is the number of experimental observations and  $P$  is the number of parameters to be fitted. The value of  $GOF^{48,50}$  is given by,

$$GOF = R_{wp} / R_{exp} \quad (10)$$

Although the  $R$  values are useful indicators for evaluation of a refinement, they should not be overinterpreted. The most important criteria for judging the quality of the Rietveld refinement are the matching of the calculated pattern to the observed data and the chemical sense of the structural model. The former can be evaluated on the basis of the final profile plot using the complete range of data collected, and the latter on a critical examination of the final atomic parameters, interatomic bond distances and bond angles.

## 6 Review of X-Ray Analysis of Kidney Stones

The classic paper on the mineralogy of human kidney stones by Prien & Frondel<sup>51</sup> focused on the identification of mineral phases in urinary stones. Similarly, the studies on X-ray powder analysis of kidney stones by Lonsdale,<sup>52</sup> Sutor et al.,<sup>53</sup> Gibson,<sup>54</sup> and Mansfield & Griffith<sup>55</sup> are primarily concerned with the qualitative mineralogy of human kidney stones. Powder X-ray analysis of first large group of stones by Herring<sup>56</sup> showed the presence of whewellite in 43% and weddellite in 61% of the stones. This was surprisingly the only report to mention weddellite as the most frequent form of calcium oxalate in human kidney stones. Several extensive

studies on the frequency of occurrence of different crystalline phases in kidney stones from various locations in Europe, the United States, Canada and South Africa have been performed using the powder XRD method.<sup>57-59</sup> On the basis of XRD analysis of 5035 stones from the population in Germany, Leusmann<sup>58</sup> found whewellite in 70% and weddellite in 44% of the samples. Murphy & Pyrah<sup>57</sup> in a survey of 250 mixed kidney stones retrieved from patients in U.K. showed that hydroxyapatite (APP) occurs with greatest frequency (32%) followed by whewellite (31%), struvite (14%) and weddellite (13%). Results of XRD analysis of American populations<sup>35</sup> also revealed APP as the frequent component (26%) with whewellite and weddellite together comprising of about 31%. Laing & Kerr<sup>59</sup> analyzed more than 3000 kidney stones from South African population and found a high prevalence of whewellite and weddellite phases (83% in total) with APP found in only 5% of the renal stones. A similar study with 1816 kidney stones<sup>60</sup> from Japan indicated that whewellite and weddellite can account for about 82% of total stone samples with a high percentage of uric acid/urate stones (~16%). The composition analysis of 1050 kidney stones from an Indian population by Ansari et al.<sup>11</sup> showed that the most frequently found constituent was whewellite (80%) followed by weddellite (20%); apatite, struvite and uric acid together accounted for about 5% of the stones. Findings from other locations around the world all show variation in both the incidence of stone formation for the population and a variation in the relative abundance of various phases. It should be emphasized that all compositional analyses of kidney stones as mentioned above utilized the traditional powder XRD method for identification of crystalline phases in urinary stones. For an accurate quantitative analysis of constituent phases in kidney stones it is, however, necessary to perform the Rietveld refinement using high quality X-ray powder diffraction data.

## 7 Rietveld Analysis of Kidney Stones

Quantitative phase analysis of kidney stones using the Rietveld method has been limited to very few reports in the literature. Daudon et al.<sup>14</sup> applied the Rietveld technique with neutron powder diffraction data to study the whewellite kidney stones. The Rietveld analysis with X-ray powder diffraction data by Orlando et al.<sup>8</sup> established quantitative phase estimates in two multi-phase kidney stones of patients from Brazil. Results of our study on the structural and micro-structural characterization of human kidney stone using the Rietveld analysis have been described

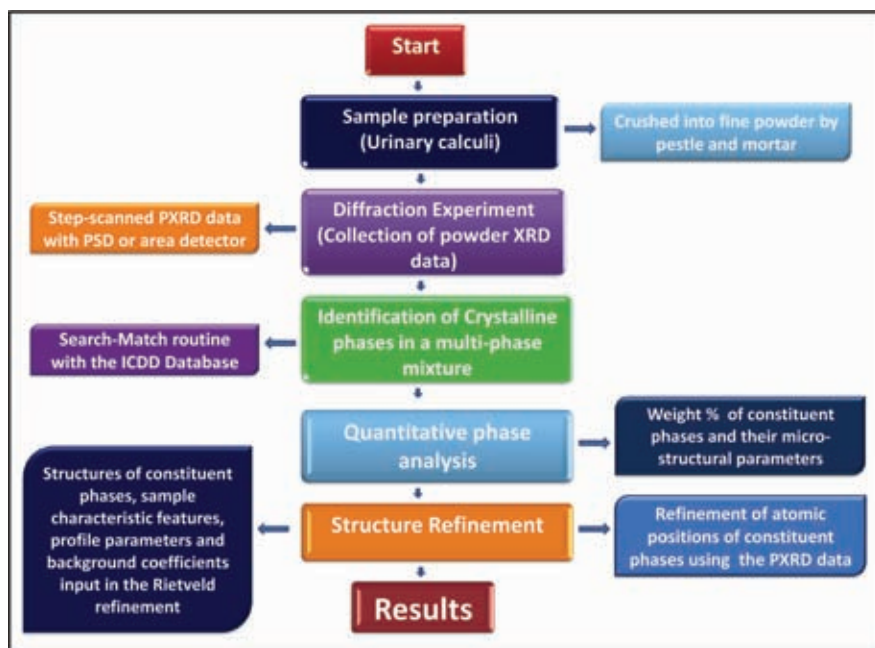


in a recent publication by Ghosh et al.<sup>45</sup> Urinary calculi used in the study were made available to us via normal surgery, i.e., following the standard ethical procedures, from patients admitted to the SSKM Hospital, Kolkata, India. The dry calculi samples (KS1-KS10) of varying sizes (2–21 mm) were crushed into fine powders using an agate pestle and mortar for X-ray analysis. High quality X-ray powder diffraction data were collected on a D8 Advance diffractometer (Bruker AXS, Karlsruhe, Germany) using the Bragg-Brentano para-focusing geometry and  $\text{CuK}\alpha$  radiation ( $\lambda = 1.5418 \text{ \AA}$ ). The XRD data were recorded at room temperature (295K) with a step size of  $0.02^\circ$  ( $2\theta$ ) and counting time of 25 s per step over an angular range  $6^\circ < 2\theta < 80^\circ$ .

The first step for quantitative analysis of urinary calculi is the identification of crystalline phases in the XRD pattern using the Powder Diffraction Database and a standard search-match software. In the present analysis, ICDD PDF2 (release 2003) was used and the presence of calcium oxalate monohydrate (COM, PDF-10-075-1313), calcium oxalate dihydrate (COD, PDF-10-075-1314), calcium hydroxyapatite (APP, PDF-00-001-1008), anhydrous uric acid (UAA, PDF-00-019-1995) and ammonium acid urate (AAU)<sup>61</sup> was established in the calculi samples KS1-KS10. The Rietveld refinement was carried out for quantitative phase analysis and micro-structural characterization of constituent phases using the MAUD program.<sup>62</sup> A diffraction pattern is simulated from a series of structural

(lattice parameters, atomic coordinates, occupancy factors, displacement parameters etc.) and micro-structural (crystallite sizes and r.m.s. lattice micro-strain) parameters, the sample characteristic features (preferred orientation, residual stress, sample thickness, absorption etc.) as well as the profile parameters and background coefficients. The simulated powder pattern is then compared with the experimental powder diffraction profile through an iterative least-squares procedure via minimization of residual parameters as describe earlier.<sup>41,50</sup>

The peak profiles are fitted using the pseudo-Voigt functions<sup>48,49</sup> with an asymmetry correction at low angle. The background can be described by a suitable polynomial function. Initially, the scale factor, zero shift ( $2\theta$ ), background coefficients and profile parameters are refined. In the next stage, the structural and micro-structural parameters of the constituent phases are alternately refined along with the earlier parameters. The occupancy factors and isotropic displacement parameters are normally held fixed at the stoichiometric values and  $B_{\text{iso}}$ , respectively, obtained from the corresponding single-crystal structure analysis. The starting atomic coordinates and isotropic displacement parameters are taken from the related literatures.<sup>61,63–65</sup> Micro-strain parameters are evaluated using the POPA (1998)<sup>66</sup> anisotropic model as incorporated in the MAUD program. Different steps of structural and micro-structural characterization of kidney stones using powder XRD method are shown in Scheme 1.



**Scheme 1:** Schematic view of different steps for kidney stone analysis using PXRD.

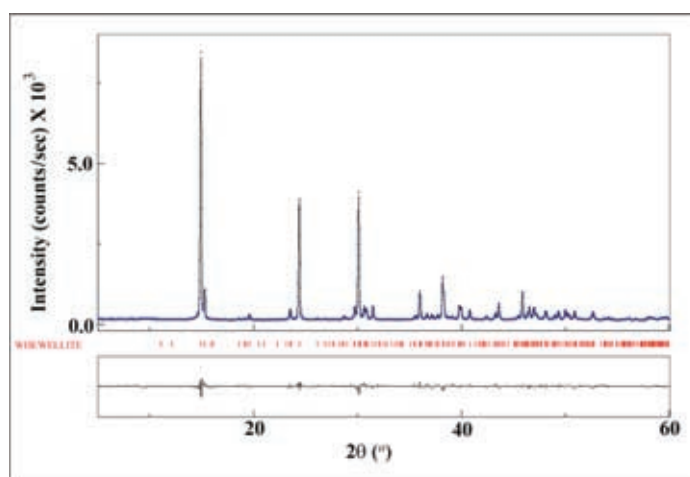
## 8 Results and Discussion

The results of Rietveld refinements of calculi samples KS1-KS10, along with the histories of the patients, are summarized in Table 1. The

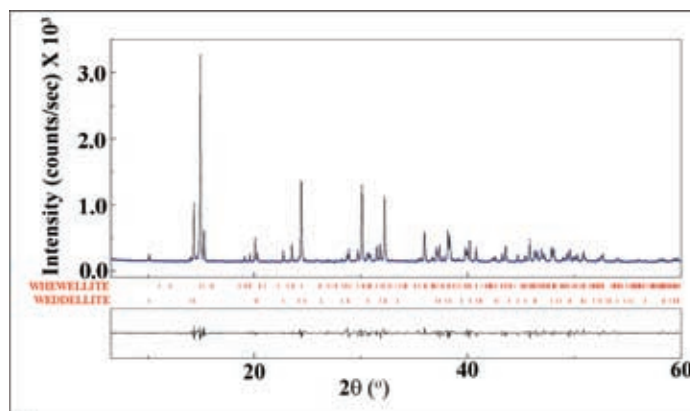
agreements between the observed and calculated powder patterns of selected urinary calculi (KS1 and KS4) are shown in Figures 1a and 1b, respectively, which clearly indicate that irrespective of

**Table 1:** Rietveld refinement parameters of samples KS1-KS10 with patient history.

Sample	Gender	Stone Size (mm)	Age	Constituent phases (wt %)					$R_p$	$R_{wp}$	$R_{exp}$
				COM	COD	APP	UAA	AAU			
KS1	Male	21	40	100					0.0418	0.0564	0.0713
KS2	Male	6–10	15	100					0.0409	0.0575	0.0861
KS3	Male	2–5	14	100					0.0342	0.0473	0.07764
KS4	Female	3–7	19	59.9	40.1				0.0433	0.0640	0.0800
KS5	Female	18	40	98.1		1.9			0.0433	0.0613	0.0799
KS6	Female	7–10	30	83.8		16.2			0.0509	0.0773	0.0887
KS7	Male	6–9	37	82.7		17.3			0.0497	0.0683	0.0887
KS8	Male	4–7	21	45.7	53.0	1.3			0.0759	0.1108	0.0762
KS9	Female	14	72	84.7			15.3		0.0632	0.0829	0.0364
KS10	Female	3–8	38	63.0			26.5	10.5	0.0470	0.0683	0.0289



(a)



(b)

**Figure 1:** Final Rietveld plot of (a) KS1 and (b) KS4 samples with observed (blue cross), calculated (black) and difference (black) profiles.

**Table 2:** Refined unit cell dimensions and microstructural parameters of the constituent phases of urinary calculi samples.

Sample	Phase	Unit Cell Dimensions					Crystallite size (nm)	Microstrain
		a(Å)	b(Å)	c(Å)	$\alpha(^{\circ})$	$\beta(^{\circ})$		
KS1	COM	6.2938(1)	14.5918(2)	10.1218(2)		109.471(2)	100(2)	0.032(3)
KS2	COM	6.2952(1)	14.5904(2)	10.1201(2)		109.460(1)	100(2)	0.080(2)
KS3	COM	6.2915(1)	14.5849(2)	10.1179(1)		109.469(2)	96(2)	0.136(2)
KS4	COM	6.2945(1)	14.5952(3)	10.1191(3)		109.477(2)	117(2)	0.087(3)
	COD	12.3645(2)		7.3564(2)			134(4)	0.084(4)
KS5	COM	6.2970(1)	14.5983(2)	10.1248(2)		109.461(2)	124(2)	0.110(4)
	APP	9.3997(1)		6.9298(2)			42(4)	0.060(3)
KS6	COM	6.2952(1)	14.5976(2)	10.1215(3)		109.470(2)	123(2)	0.108(2)
	APP	406(2)		6.879(1)			31(5)	0.25(4)
KS7	COM	6.2935(2)	14.5940(2)	10.1212(2)		109.484(1)	97(6)	0.109(2)
	APP	9.441(8)		6.875(6)			14(2)	0.13(1)
KS8	COM	6.2955(2)	14.5987(2)	10.1249(3)		109.491(4)	168(3)	0.136(2)
	COD	12.3802(4)		7.3591(3)			105(3)	0.103(5)
	APP	9.372(2)		6.872(2)			100(4)	0.44(3)
KS9	COM	6.2945(1)	14.5905(3)	10.1212(2)		109.473(2)	146(5)	0.008(2)
	UAA	14.471(2)	7.435(1)	6.203(2)		65.11(2)	103(2)	0.009(7)
KS10	COM	6.2943(2)	14.5921(5)	10.1223(6)		109.47(4)	157(4)	0.008(2)
	UAA	14.457(1)	7.4315(4)	6.206(6)		65.062(6)	210(3)	0.002(3)
	AUU	3.632(2)	10.111(7)	10.597(6)	113.22(4)	92.25(7)	93.33(4)	228(2)

the number of constituent phases and their quantities, the Rietveld analysis is an effective approach for structural and micro-structural characterization of kidney stones. The refined cell parameters of constituent phases and their micro-structural parameters are listed in Table 2. The observed cell parameters of constituent phases in KS1-KS10 do not differ significantly from the values reported for whewellite,<sup>14,63</sup> weddellite,<sup>63</sup> anhydrous uric acid<sup>65</sup> and ammonium hydrogen urate<sup>61</sup> on the basis of single crystal structure analysis. The quantitative phase analysis using the Rietveld whole powder profile-fitting structure refinement method showed that KS1-KS3 samples are monophasic (COM), while other urinary calculi (KS4-KS10) are mixture of phases. The COM is the major constituent (63.0–98.1 wt%) in KS5-KS7, KS9 and KS10, while the amounts of COD phase in KS4 and KS8 are 40.1 and 53.0 wt%, respectively. Other minor phases present were APP (1.3–17.3 wt%) in KS5-KS8, UAA (15.3–26.5 wt%) in KS9, KS10 and AAU (10.5 wt%) in KS10. The results of quantitative phase analysis of KS1-KS10 are in agreement with that reported earlier,<sup>7,67</sup> which indicated that COM is the primary composition in majority of

kidney stones retrieved from patients in the Indian sub-continent.

Since the composition of KS1, KS2 and KS3 is 100% COM, it is worth comparing their structural features as obtained from the present Rietveld analysis with those reported earlier using single crystal X-ray analysis of whewellite (COM).<sup>63</sup> The coordination geometry around the two symmetry-independent Ca atoms, both coordinated to eight O atoms, in the asymmetric unit of COM in KS1 can be best described as a distorted square antiprism. Seven of these O atoms are from oxalate ions and the eighth oxygen atom belongs to the water molecule. The Ca-O distances lie in the range 2.372(2) Å to 2.508(1) Å with the Ca1-Ca2 separation of 3.832(2) Å. The observed bond distances and bond angles of COM in KS1 are comparable with the corresponding values reported in the literature.<sup>14,63</sup> The adjacent Ca-centered polyhedra of COM in KS1 are edge fused to form two-dimensional molecular sheets parallel to the (100) plane (Fig. 2a). The oxalate groups lying in the (010) plane and lattice water molecules interlink the two-dimensional sheets of COM into a three-dimensional framework structure (Fig. 2b).

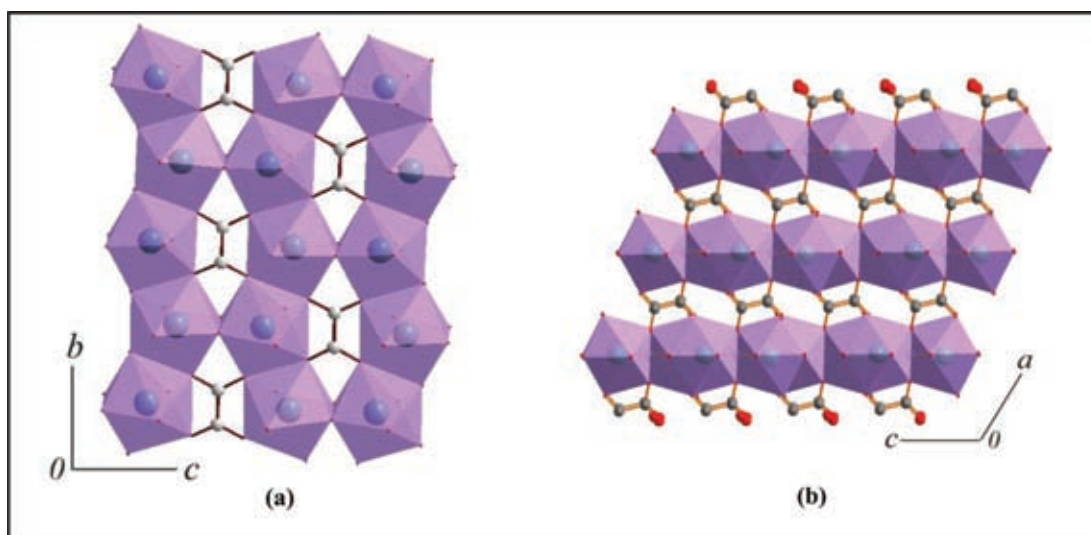


**Figure 2:** View of COM structure, projected on to (a) the (100) plane and (b) the (010) plane.

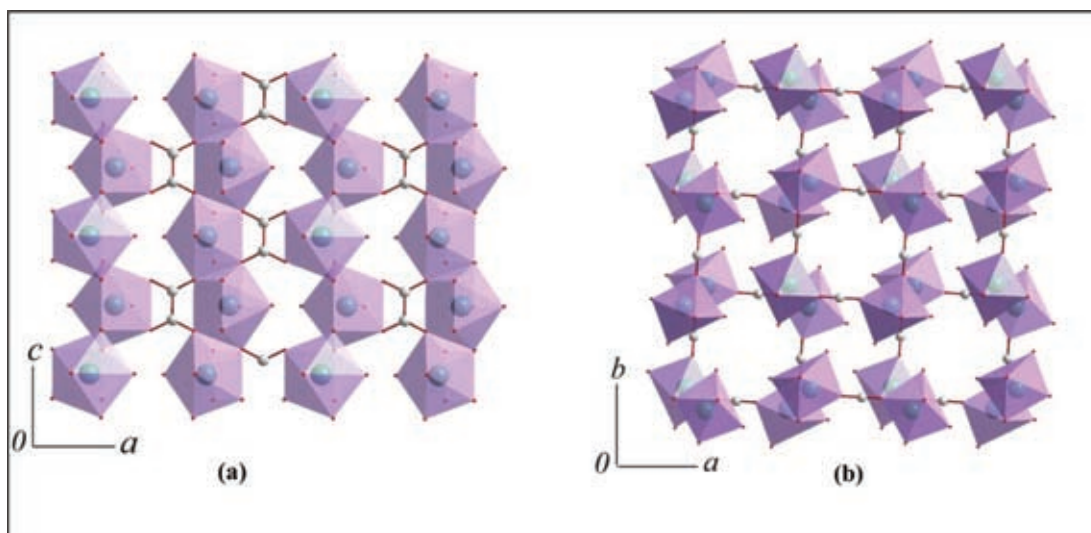


**Figure 3:** View of COD structure, projected on to (a) the (010) plane and (b) the (001) plane.

The structure of the COD phase in the KS4 and KS8 samples resembles the weddellite structure reported in the literature.<sup>63</sup> The calcium coordination polyhedron in the COD structure is built up by eight O atoms, six of them belonging to oxalate ions and the remaining two to water molecules. The observed Ca-O bond distances in KS8, ranging between 2.67(2) and 2.36 (1) Å, agree with the corresponding values reported earlier.<sup>63</sup> Unlike the COM structure, in which the calcium polyhedra generate a molecular sheet in the (100) plane, the calcium polyhedra in the COD structure are edge-fused to two adjacent polyhedra to form one-dimensional chains running along the [001] direction (Fig. 3a). Further linking of these chains through the oxalate moieties results

in a three-dimensional network consisting of  $6.23 \times 6.23$  Å square frames (Fig. 3b).

## 9 Conclusions

Among the various chemical and physical methods that can be used to study urinary calculi, X-ray powder diffraction coupled with the Rietveld analysis can provide an accurate estimate of quantitative phase abundance in human kidney stones. Quantitative phase analysis of ten (10) urinary calculi (KS1-KS10) retrieved from patients of eastern India indicates that whewellite (COM) is the major constituent phase in most of the stones. Three stone samples (KS1-KS3) were composed of exclusively calcium oxalate monohydrate (whewellite) phase, whereas the remaining seven



calculi samples (KS4-KS10) showed the presence of mixed crystalline phases with whewellite (45.7–98.1 wt%), weddellite (40.1–53.0 wt%), calcium hydroxyapatite (1.3–17.3 wt%), ammonium acid urate (10.5 wt%) and anhydrous uric acid (15.3–26.5 wt%). The Rietveld structure refinements of whewellite in KS1 and weddellite in KS8 reveal a three-dimensional framework built via interlinking of calcium polyhedra through oxalate moieties and lattice water molecules. The whewellite nanocrystals in the urinary calculi analysed in the present study have the same structure at the atomic level and almost the same size at the nanometric scale.

### Acknowledgements

The author wishes to thank Dr. S. Chakraborty, SSKM Hospital, Kolkata, India for providing samples. The author is grateful to Prof. Monika Mukherjee, Dr. Soumen Ghosh, Dr. Dipak K. Hazra, Mr. Abir Bhattacharya, Mr. Uday Das, Mrs. Paramita Chatterjee and Ms. Tanusri Dey for useful discussions. Financial assistance through the grant (No. SR/ S2/ CMP-75/ 2012) from the Department of Science and Technology (DST), Govt. of India, New Delhi, is gratefully acknowledged.

Received 12 November 2013.

### References

- Williams, J. C. (2009) *Br. J. Urol.* **104**, 8.
- Knoll, T. (2007) *Eur. Urol. Suppl.* **6**, 717.
- Bazin, D., Daudon, M., Combes, C. & Rey, C. (2012) *Chem. Rev.* **112**, 5092.
- Taylor, E. N. & Curhan, G. C. (2006) *Kidney Int.* **70**, 835.
- Coe, F. L., Evan, A. & Worcester, E. (2005) *J. Clin. Invest.* **115**, 2598.
- Sperrin, M. W. & Rogers, K. (1998) *Br. J. Urol.* **82**, 781.
- Satish, R. S., Ranjit, B., Ganesh, K. M., Rao, G. N. & Janardhana, C. (2008) *Curr. Sci.* **94**, 104.
- Orlando, M. T. D., Kuplich, L., de Souza, D. O., Belich, H., Depianti, J. B., Orlando, C. G. P., Medeiros, E. F., da Cruz, P. C. M., Martinez, L. G., Corrêa, H. P. S. & Ortiz, R. (2008) *Powder Diffr. Suppl.* **23**, S59.
- Daudon, M., Jungers, P. & Bazin, D. (2008) *New Engl. J. Med.* **359**, 100.
- Pak, C. Y. C. (2008) *J. Urol.* **180**, 813.
- Ansari, M. S., Gupta, N. P., Hemal, A. K., Dogra, P. N., Seth, A., Aron, M. & Singh, T. P. (2005) *Int. J. Urol.* **12**, 12.
- Sarika, K., Altay, B. & Erturhan, S. (2008) *Urol.* **71**, 771.
- Taylor, E. N., Stampfer, M. J. & Curhan, G. C. (2005) *J. Am. Med. Assoc.* **293**, 455.
- Daudon, M., Bazin, D., André, G., Jungers, P., Cousson, A., Chevallier, P., Véron, E. & Matzen, G. (2009) *J. Appl. Cryst.* **42**, 109.
- Coe, F. L., Parks, J. H. & Asplin, J. R. (1992) *N. Engl. J. Med.* **327**, 1141.
- Taylor, E. N., Stampfer, M. J. & Curhan, G. C. (2004) *J. Am. Soc. Nephrol.* **15**, 3225.
- Gracia-Garcia, S., Millan-Rodriguez, F., Rousaud-Baron, F., Montanes-Bermudez, R., Angerri-Feu, O., Sanchez-Martin, F., Villavicencio-Mavrich, H. & Oliver-Samper, A. (2011) *Actas. Urol. Esp.* **35**, 354.
- Rule, A. D., Bergstralh, E. J., Melton, L. J., Li, X., Weaver, A. L. & Lieske, J. C. (2009) *Clin. J. Am. Soc. Nephrol.* **4**, 804.
- Caudarella, R., Vescini, F., Buffa, A., La Manna, G. & Stefoni, S. (2004) *Urol. Int.* **72**, 17.
- Cytron, S. E., Kravchick, S., Ben-ami, S., Shulzinger, E., Vasserman, I., Raichlin, Y. & Katzir, A. (2003) *Urology.* **61**, 231.
- Daudon, M., Bazin, D., Adil, K. & Le Bail, A. (2011) *Acta. Cryst.* **E67**, o1458.
- Kasidas, G. P., Samuell, C. T. & Weir, T. B. (2004) *Ann. Clin. Biochem.* **41**, 91.
- Miller, L. M. & Dumas, P. (2006) *Biochem. Biophys. Acta.* **1758**, 846.
- Singh, I. (2008) *Int. Urol. Nephrol.* **40**, 595.
- Schubert, G. (2006) *Urol. Res.* **34**, 146.
- Harada, Y., Tomita, T., Kokubo, Y., Daimon, H. & Ino, S. (1993) *J. Elec. Micros.* **42**, 294.
- Lee, H. P., Leong, D. & Heng, C. T. (2011) *Urol. Res.* **39**, 1.
- Fazil, M. Y. M., Lekshmi, P. R., Varma, L. & Koshy, P. (2009) *Urol. Res.* **37**, 277.
- Uvarov, V., Popov, I., Shapur, M., Abdin, T., Gofrit, O. N., Podes, D. & Duvdevani, M. (2011) *Environ. Geochem. Health.* **33**, 613.
- Carmona, P., Bellanato, J. & Escolar, E. (1997) *Biospectroscopy.* **3**, 331.
- Pestaner, J. P., Mullick, F. G., Johnson, F. B. & Centeno, J. A. (1996) *Arch. Pathol. Lab. Med.* **120**, 537.
- Hong, T. D., Phat, D., Plaza, P., Daudon, M. & Dao, N. Q. (1992) *Clin. Chem.* **38**, 292.
- Daudon, M., Bader, C. A. & Jungers, P. (1993) *Scann. Micros.* **7**, 1081.
- Khan, S. R. & Hackett, R. L. (1986) *J. Urol.* **135**, 818.
- Kim, K. M. (1982) *Scann. Electron Micros.* **4**, 1635.
- Frost, R. L. & Weier, M. L. (2004) *Thermochim. Acta.* **409**, 79.
- Frost, R. L. & Weier, M. L. (2003) *Thermochim. Acta.* **406**, 221.
- Cullity, B. D. *Elements of X-ray Diffraction*, 2nd Ed; Addison-Wesley Pub. Co. Inc., USA. 1978.
- Rietveld, H. M. (1967) *Acta Cryst.* **22**, 151.
- Rietveld, H. M. (1969) *J. Appl. Cryst.* **2**, 65.
- Young, R. A. (1996) Editor. *The Rietveld Method*, IUCr/ Oxford University Press.
- Hill, R. J. & Howard, C. J. (1987) *J. Appl. Cryst.* **20**, 467.
- Bish, D. L. & Howard, S. A. (1988) *J. Appl. Cryst.* **21**, 86.
- Reid, J. W. & Hendry, J. A. (2006) *J. Appl. Cryst.* **39**, 536.
- Ghosh, S., Basu, S., Chakraborty, S. & Mukherjee, A. K. (2009) *J. Appl. Cryst.* **42**, 629.

46. Chung, F. H. (1974) *J. Appl. Cryst.* **7**, 519.
47. Hubbard, C. R., Evans, E. H. & Smith, D. K. (1976) *J. Appl. Cryst.* **92**, 169.
48. Young, R. A. & Wiles, D. B. (1982) *J. Appl. Cryst.* **15**, 430.
49. Enzo, S., Fagherazzi, G., Benedetti, A. & Polizzi, S. (1988) *J. Appl. Cryst.* **21**, 536.
50. Lutterotti, L., Scardi, P. & Maistrelli, P. (1992) *J. Appl. Cryst.* **25**, 459.
51. Prien, E. L. & Frondel, C. (1947) *J. Urol.* **57**, 949.
52. Lonsdale, K. (1968) *Nature*, **159**, 1199.
53. Sutor, D. J., Wooley, S. E. & Illingworth, J. J. (1974) *Br. J. Urol.* **46**, 393.
54. Gibson, R. I. (1974) *Am. Mineral.* **59**, 1177.
55. Mansfield, C. F. & Griffith, D. P. (1976) *Am. Mineral.* **61**, 1031.
56. Herring, L. C. (1962) *J. Urol.* **88**, 545.
57. Murphy, B. T. & Pyrah, L. N. (1962) *Br. J. Urol.* **34**, 129.
58. Leusmann, D. B. (1991) *Scand. J. Urol.* **25**, 141.
59. Laing, M. & Kerr, A. (1991) *South Afr. Med. J.* **79**, 407.
60. Hossain, R. Z., Ogawa, Y., Hokama, S., Morozumi, M. & Hatano, T. (2003) *Int. J. Urol.* **10**, 411.
61. Fridel, P., Bergmann, J., Kleeberg, R. & Schubert, G. (2006) *Z. Kristallogr. Suppl.* **23**, 517.
62. Lutterotti, L. (2008) MAUD. Version 2.064. <http://www.ing.unitn.it/~maud/>.
63. Tazzoli, V., & Domeneghetti, C. (1980) *Am. Mineral.* **65**, 327.
64. Sudarsanan, K. & Young, R. A. (1969) *Acta Cryst.* **B25**, 1534.
65. Ringertz, H. (1966) *Acta. Cryst.* **20**, 397.
66. Popa, N. C. (1998) *J. Appl. Cryst.* **31**, 176.
67. Chandrajith, R., Wijewardana, G., Dissanayake, C. B. & Abeygunasekara, A. (2006) *Environ. Geochem. Health*, **28**, 393.



**Dr. Alok K. Mukherjee** is a graduate of the University of Calcutta (B.Sc., 1969). After Ph.D. (Sc) in 1977 from Visva-Bharati University, Santiniketan, he joined National Physical Laboratory, New Delhi. In 1981, he moved to Jadavpur University, Kolkata, where he is currently a Professor in the Department of Physics. The research activity of Prof. Mukherjee covers several aspects of structural crystallography with present emphasis on the application of X-ray powder diffraction for solving crystal structures of molecular solids and microstructural characterization of mineral deposits in human kidney and gall-bladder stones. He is in the editorial board of different national and international journals and at present a member of the Executive Committee of International Union of Crystallography Commission on Powder Diffraction. He has published more than 130 research papers in various international journals.